Research Article

Rabiye Uslu Erdemir, Gokhan Kilic, Duygu Sen Baykal, Ghada ALMisned, Shams A. M. Issa, Hesham M. H. Zakaly, Antoaneta Ene*, Huseyin Ozan Tekin*

Diagnostic and therapeutic radioisotopes in nuclear medicine: Determination of gamma-ray transmission factors and safety competencies of high-dense and transparent glassy shields

https://doi.org/10.1515/chem-2022-0167
received April 16, 2022; accepted May 9, 2022

Abstract: We present the findings of an extensive examination on newly designed CdO-rich and transparent glass shields for nuclear medicine facilities in lieu of traditional and unfavorable materials, such as lead and concrete. Gamma-ray transmission factors of newly designed glass shields are determined using a variety of diagnostic, therapeutic, and research radioisotopes, including ^{67}Ga, ^{57}Co, ^{111}In, ^{201}Tl, ^{99m}Tc, ^{51}Cr, ^{131}I, ^{58}Co, ^{137}Cs, ^{133}Ba, and ^{60}Co. A general-purpose Monte Carlo code MCNPX (version 2.7.0) is used to determine the attenuation parameters of different material thicknesses. Next, the findings are compared using a standard concrete shielding material. The results indicate that adding more CdO to the glass composition improves the overall gamma-ray attenuation properties. As a result, among the heavy and transparent glasses developed, the C40 sample containing 40% CdO exhibited the best gamma-ray absorption properties against all radioisotopes. Furthermore, the gamma-ray absorption characteristics of this created high-density glass were shown to be better to those of a standard and heavy concrete sample. It can be concluded that the newly developed CdO-rich and transparent glass sample may be used in medical radiation fields where the radioisotopes examined are used in daily clinical and research applications.

Keywords: nuclear medicine, radioisotopes, gamma-ray, MCNPX, nuclear safety

*** Corresponding author: Antoaneta Ene,** Department of Chemistry, Physics and Environment, INPOLDE Research Center, Faculty of Sciences and Environment, Dunarea de Jos University of Galati, 47 Domneasca Street, 800008 Galati, Romania, e-mail: antoaneta.ene@ugal.ro
*** Corresponding author: Huseyin Ozan Tekin,** Department of Medical Diagnostic Imaging, College of Health Sciences, University of Sharjah, 27272, Sharjah, United Arab Emirates; Computer Engineering Department, Istinye University, Faculty of Engineering and Natural Sciences, Istanbul 34396, Turkey, e-mail: tekin765@gmail.com
Rabiye Uslu Erdemir: Department of Nuclear Medicine, Zonguldak Bülent Ecevit University of Medicine, Zonguldak, Turkey
Gokhan Kilic: Department of Physics, Eskisehir Osmangazi University, Faculty of Science and Letters, Eskişehir, Turkey
Duygu Sen Baykal: Istanbul Kent University, Vocational School of Health Sciences, Department of Medical Imaging Techniques, Istanbul, 34433, Turkey
Ghada ALMisned: Department of Physics, College of Science, Princess Nourah Bint Abdulrahman University, P.O. Box 84428, Riyadh 11671, Saudi Arabia
Shams A. M. Issa: Physics Department, Faculty of Science, University of Tabuk, Tabuk 47512, Saudi Arabia; Physics Department, Faculty of Science, Al-Azhar University, Assiut 71524, Egypt
Hesham M. H. Zakaly: Physics Department, Faculty of Science, Al-Azhar University, Assiut 71524, Egypt; Institute of Physics and Technology, Ural Federal University, 620002 Ekaterinburg, Russia

1 Introduction

Nuclear medicine is a field of research in which radioisotope-containing medications are used to diagnose and treat diseases [1]. It began in the 1950s with the use of 131-Iodine for thyroid cancer detection and treatment. Nuclear medicine techniques are extremely effective, reliable, and painless. They involve administering a small amount of radioisotope material or radiopharmaceuticals (inorganic compounds labeled with radioisotopes, organic compounds, peptides, proteins, monoclonal antibodies and fragments, and oligonucleotides) to the patient to examine the physiological and molecular processes occurring in the body. On the other hand, gamma-rays generated by radioisotopes administered to patients are detected in nuclear medicine using planar or tomographic

technologies, such as gamma camera, single photon emission tomography (SPECT), positron emission tomography (PET), and hybrid systems (SPECT/CT, PET/CT). Diseases are diagnosed using the images generated as a consequence of processing [2,3]. In nuclear imaging, radioisotope-labeled carriers are used as noninvasive diagnostic tools to offer information on the function and structure of tissues and their surroundings [4]. All radioisotopes used in nuclear medicine are synthetic, and they are manufactured in a variety of ways, including fission in the reactor, thermal neutrons in the reactor, generator-made radioisotopes, and cyclotron-produced radioisotopes [1]. Radioisotopes are utilized in nuclear medicine for two purposes, such as therapy and diagnostics. While radioisotopes that generate electromagnetic gamma radiation are utilized for imaging, radioisotopes that are heavier, have a larger ionization energy, and decay by scattering beta- or alpha-rays with a particulate nature are employed for therapy. Meanwhile, nuclear medicine is an intentional exposure to radiation. While ionizing radiation travels through living tissue, it transfers part or all of its energy to the tissue, resulting in recognized detrimental effects on live creatures at low to high exposure levels. These are stochastic (cancer, mutations) and deterministic (tissue responses) consequences (such as dermatitis, cataract). It is critical to maintain radiation workers and the general public's exposure to radiation below safe dosage limits to avoid undiscovered negative consequences. ALARA (as low a dose as reasonably attainable) and ALARP (as low a dose as reasonably practical) principles, as well as dosage limitations established for the profession and society by international and national atomic energy institutes, and radiation safety legislation, should be obeyed [3]. With the introduction of novel targeted radioisotopes for treatment, particularly for malignant disorders, radioisotope therapy is increasingly used in nuclear medicine clinics [4]. As a result, while building nuclear medicine units, certain objectives should be defined based on time, distance, and shielding parameters to minimize radiation exposure to both personnel and patients. These objectives include assuring the safety of radioactive sources, maximizing employee, patient, and public exposure, maintaining complete control over radioisotope/radiopharmaceutical activities, and avoiding contamination spread [5–7]. Therefore, the scientific community has concentrated on developing next-generation shielding materials that may provide certain advantages over conventional shielding materials in terms of avoiding those shortcomings. In this study, we presented the findings of a complete examination of newly designed CdO-rich and transparent glass shields for usage in nuclear medicine facilities in lieu of traditional and unfavorable materials, such as lead (Pb) and concrete. Gamma-ray transmission factors (TFs) of newly designed glass shields are determined using a variety of diagnostic, therapeutic, and research radioisotopes, including ^{67}Ga, ^{57}Co, ^{111}In, ^{201}Tl, ^{99m}Tc, ^{51}Cr, ^{131}I, ^{58}Co, ^{137}Cs, ^{133}Ba, and ^{60}Co. The study's findings may provide key information for optimizing shielding materials used to protect personnel and patients in units, such as nuclear medicine, that utilize medical radiation sources.

2 Materials and methods

2.1 Investigated glassy shields

Cd-doped glasses were effectively fabricated using the melt-quenching process and a range of CdO compositions (x = 0, 15, 20, 30, and 40 mol%) (see Table 1). Each oxidized chemical was separately weighed using a high-precision scale. The platinum crucible containing the solution was heated to very high temperatures during the synthesis of glass shields. The high-temperature furnace was permitted to warm up to 900°C from room temperature for the first 60 min of the procedure. Mechanical stirring was performed every 15 min throughout this time period. Each glass sample was annealed for about an hour at 380–385°C and then cooled back to room temperature (Figure 1).

2.2 Calculation of gamma-ray TFs

The absorption characteristics of materials intended for use in fields containing medical radiation, such as nuclear medicine and diagnostic radiology, against gamma-rays are significant. The reason for this is the exposure that

Table 1: Glass codes, glass compositions, thickness, and density values of glasses

Code	P_2O_5 (mol %)	TeO_2 (mol %)	ZnO (mol %)	CdO (mol %)	Density (g/cm^3)	Thickness (mm)
C0	20	30	50	—	4.41970	2.637
C15	20	30	35	15	4.65192	2.678
C20	20	30	30	20	4.72403	2.66
C30	20	30	20	30	4.87138	2.785
C40	20	30	10	40	5.01752	2.447

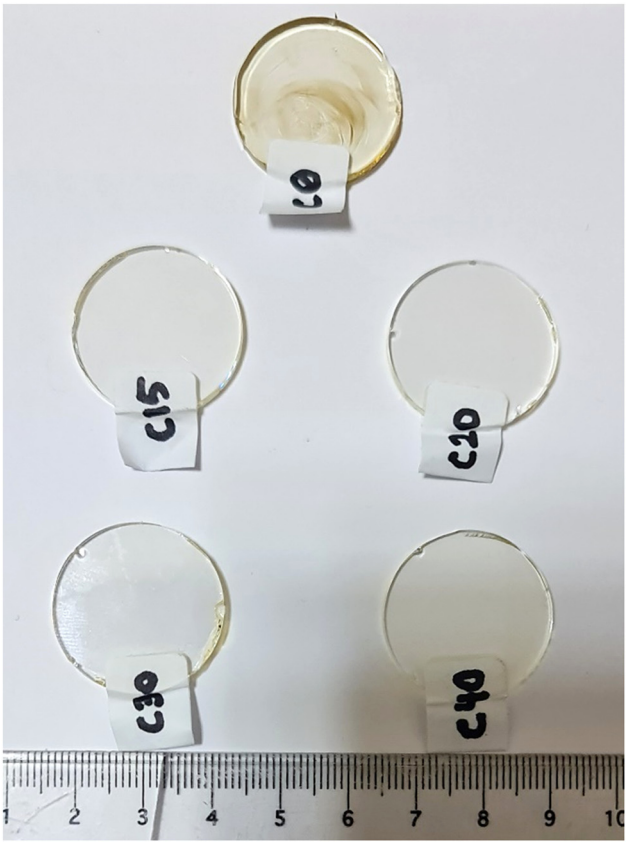

Figure 1: Synthesized glass series.

personnel working in such environments may face when dealing with the associated radiation sources, as well as the deterministic and stochastic impacts, which this exposure may have in the short and long terms [8–14]. The TF [15–17] is a critical shielding metric that is derived using the percent reduction of primary gamma-ray radiation incident on a material. It demonstrates the length dependency of the gamma-ray transmission process. Calculating TF values for a single material offers information on the degree of absorption provided by that material, while studying it for a group of materials provides critical information about the effect of changing material content on this transition factor. Thus, the direct influence of manufacturing modifications on the absorption characteristics is also well recognized. In this study, the absorption properties of CdO-based and high-density glass materials produced against some diagnostic and therapeutic radioisotopes (see Table 2) were investigated for different energies and different material thicknesses and compared with some conventional shielding materials within the framework of the same parameters. The general-purpose radiation transport code MCNPX [18] operating with the Monte Carlo simulation method was used to calculate the TF values. First, the glass structures produced were defined

Table 2: Radioisotopes and gamma-ray energies used for gamma-ray TF calculations

Radioisotope	Gamma-ray energy (MeV)
^{67}Ga	0.0086, 0.0093, 0.1840
^{57}Co	0.0144, 0.1221, 0.1365
^{111}In	0.0230, 0.1710, 0.2450
^{133}Ba	0.0532, 0.0796, 0.0810, 0.2764, 0.3029, 0.3560, 0.3838
^{201}Tl	0.0710, 0.1350, 0.1670
^{99m}Tc	0.1405
^{51}Cr	0.3201
^{131}I	0.2843, 0.3645, 0.6370, 0.7229
^{58}Co	0.5110, 0.8108
^{137}Cs	0.6617
^{60}Co	1.1732, 1.3325

according to the elemental properties given in Table 1 in the INPUT file of the MCNPX code, and their respective densities were included in the INPUT file. Then, by defining two detection areas of equal size directly in front of and behind the absorber material, fluxes of primary and secondary gamma-rays were obtained. This operation is done with the F4 definition of the MCNPX code. Finally, a source with point isotropic behaviors was located at a point before the absorber glass material and the first detection area (see Figure 2). For each simulation cycle, the source description and hence the characteristic gamma-ray energy were determined. Meanwhile, 10^8 particle counts were generated for each simulation cycle through random event generator of MCNPX. At the end of the simulation processes, the relative error rates from the OUTPUT file were observed to be less than 1%. MCNPX simulations were performed using the D00205ALLCP03 MCNPXDATA package is included of DLC-200/MCNPDATA cross-section libs (Figure 1).

3 Results and discussions

The TF values of the fabricated glass materials were calculated for 0.5, 1.5, 2.5, and 3 cm thicknesses as a function of the gamma-ray values emitted from different radioisotopes. Figure 3 depicts the TFs of investigated glasses and steel-magnetite concrete as a function of used radioisotope energy (MeV) at different glass thicknesses. As can be seen from the figure, the amount of the transmitted gamma-rays that all for glass samples and the conventional shielding materials (i.e., reinforced concrete) increased depending on the increasing radioisotope energy at all material thicknesses. Behaviorally,

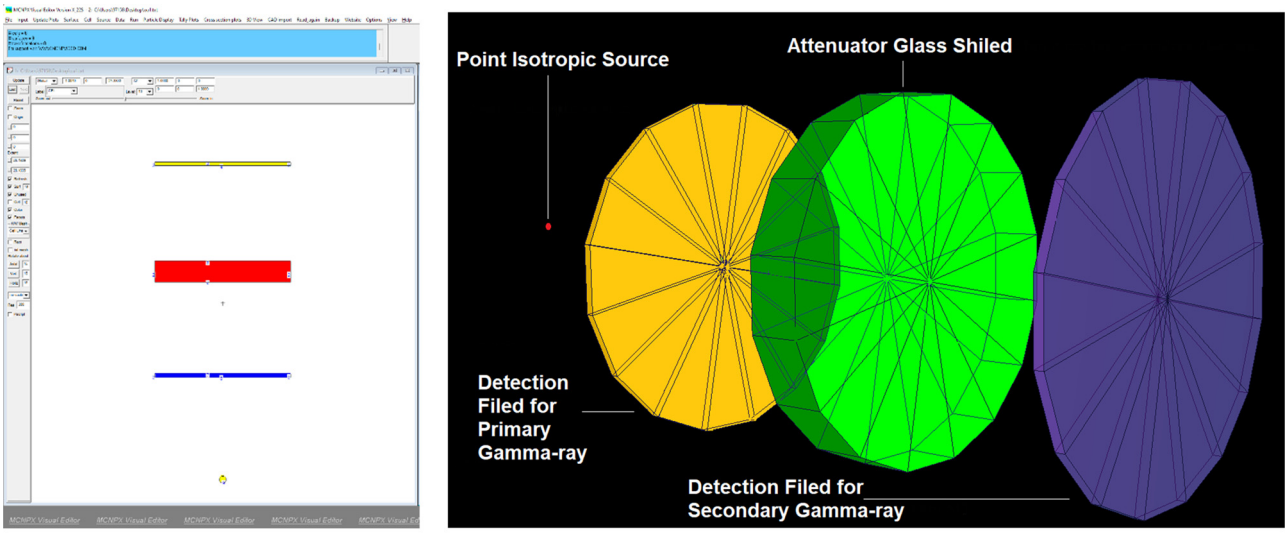

Figure 2: (a) 2-D view of designed MCNPX simulation setup. (b) 3-D illustration of designed MCNPX setup (2-D and 3-D views are obtained from MCNPX Visual Editor VisedX22S).

the common attitudes of all materials is the low transmission rate observed at low gamma-ray energies. This is due to the limited penetrating capability of low energy gamma-rays. On the other hand, for the same energy value, a certain TF value difference was observed proportionately between the material with the lowest thickness and the material with the highest thickness. This may be explained by the fact that the primary gamma-ray that penetrates the thin material does not undergo complete energy absorption. On the other hand, obtaining the lowest TF value at 3 cm, which is the thickest value for the same energy value, can be explained by the primary gamma-ray's first interaction and subsequent interactions in the material occurring at a sufficiently large thickness and simply left the material with minimal quantitative values. As a consequence, the TF values for the radioisotope energies utilized in the glass samples and the concrete material used as the reference material were lowest at low energies and high thicknesses. In the largest context, this situation is linked to the penetrating qualities of gamma-rays [19–22], and no abnormal behavior tendencies have been identified. As the second step of TF value assessment, the TF values of glass and concrete samples were compared for identical thickness values, and the material with the lowest TF value and hence the best absorption characteristics was determined. Figure 4 depicts the comparison of the TFs as a function of used radioisotope energy (MeV) for different glass thicknesses and concrete. Figure 4 also quantitatively depicts the particular gamma-ray TF behavior of all materials investigated and compared at the same thickness. The TF value of the C series glasses fabricated according to the data obtained in this phase of the investigation is proportional to the ratio of CdO added to the glass at a certain thickness. Among the glass samples developed, the C40 sample with the greatest CdO doping ratio and densest structure exhibited the lowest TF values throughout the thickness range. This may be attributed to the positive contribution of the maximum CdO solid's density rise to the gamma-ray absorption qualities. Meanwhile, the C40 sample's TF values are lower than those of the concrete with additives. This demonstrates that these next-generation materials, which outperform the absorption capabilities of currently used heavy-mixed concrete, may be employed for identical reasons. In the last comparison stage of the study, the half value layer (HVL) values of all C series glasses were compared with the reinforced concrete material. Figure 5 depicts the variations of HVL (cm) with photon energy (MeV) for all C0–C8 glasses and concrete. A material's HVL value may be defined for a given photon energy [23]. The HVL value is the material thickness necessary to quantitatively lower the intensity of photons at the relevant energy using that material [24–35]. Thus, the fact that the HVL value is low for a given photon energy value is a significant pattern of the material's exceptional absorption capabilities. As seen in the figure, the C40 sample had the lowest possible HVL values at all energy levels. As a result, employing C40 samples instead of traditional concrete shields may be advantageous in terms of physical space requirements and space costs.

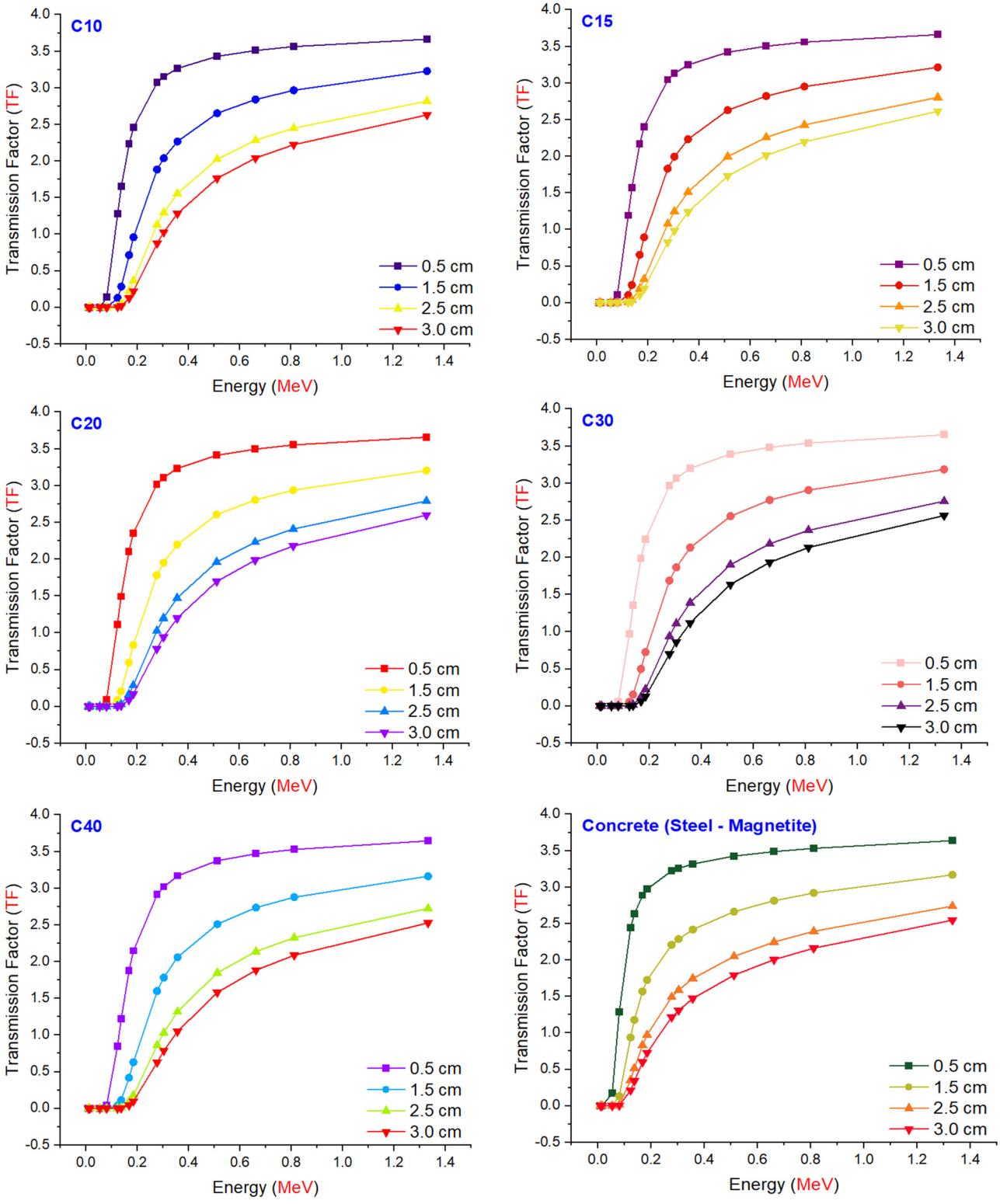

Figure 3: TFs of investigated glasses and steel-magnetite concrete as a function of used radioisotope energy (MeV) at different glass thicknesses.

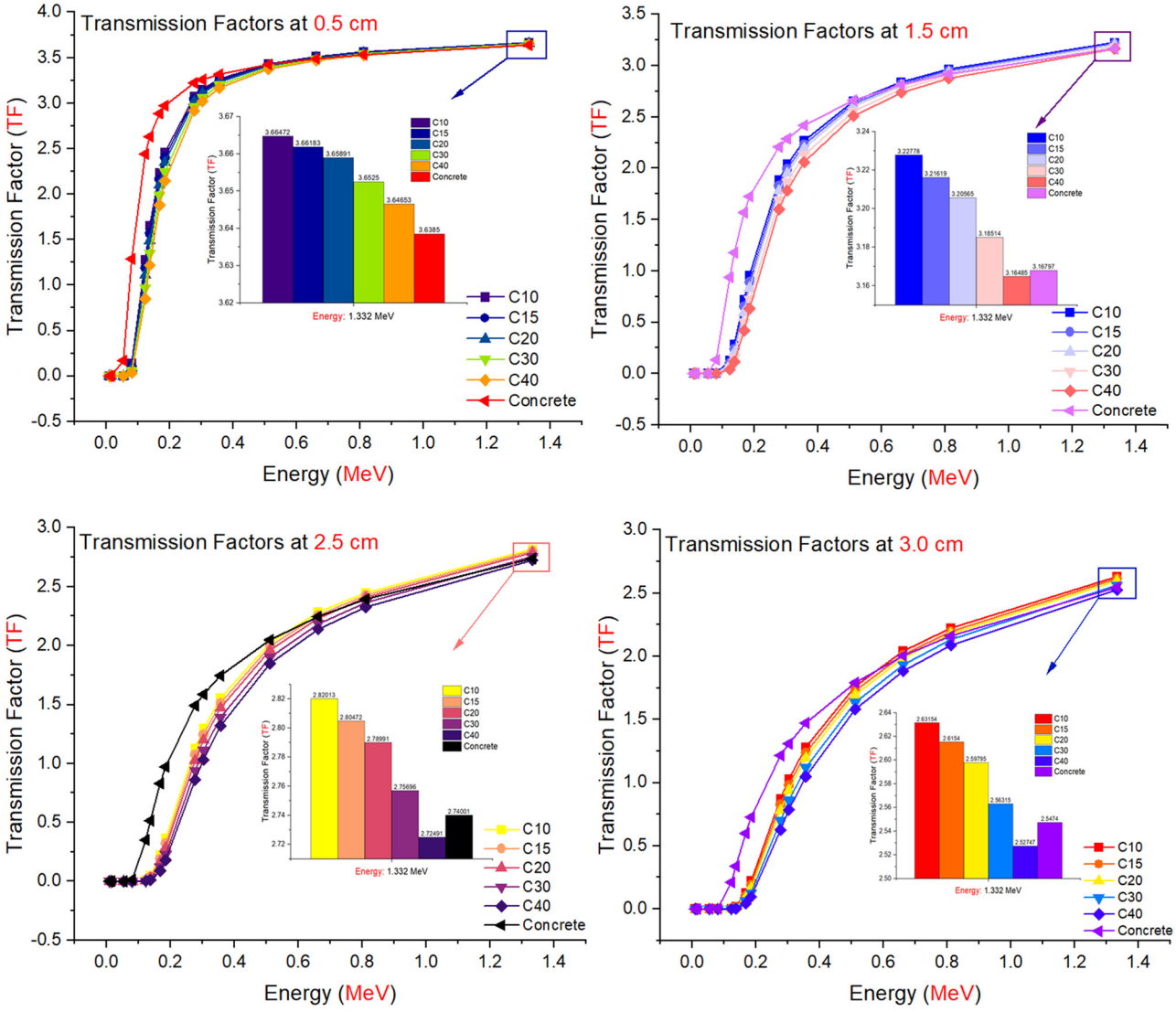

Figure 4: Comparison of the TFs as a function of used radioisotope energy (MeV) for different glass thicknesses and concrete.

4 Conclusion

One of the challenges that researchers have focused on in recent years is developing alternative, ecologically acceptable, nontoxic, and low-cost materials to substitute Pb and concrete in equipment and structural designs used in medical and industrial radiation applications. Currently, some specialized glasses are employed in a variety of configurations for a variety of purposes in nuclear and diagnostic radiology facilities. Our primary goal in this research was to observe the absorption differences across a broad radioisotope energy range caused by structural changes in the glass composition accompanied by certain chemical modifications and to investigate the relationship between these differences and the chemical modifications. The TF values of glasses synthesized utilizing the distinctive gamma-ray energies of a variety of therapeutic, diagnostic, and research radioisotopes, such as Barium, were determined for this purpose. The findings indicate that the linearly increasing CdO ratio in such a glass composition contributes positively to all gamma-ray energies. As a consequence, the C40 sample containing 40% CdO was shown to have the best absorption characteristics among the heavy and thick glasses prepared. More importantly, the gamma-ray absorption properties of this high-density glass manufactured were shown to be superior to those of conventional and heavy concrete sample. The critical point is that the transparency of the C40 sample, which exhibits superior qualities to conventional materials, allows for viewing of the radioactive

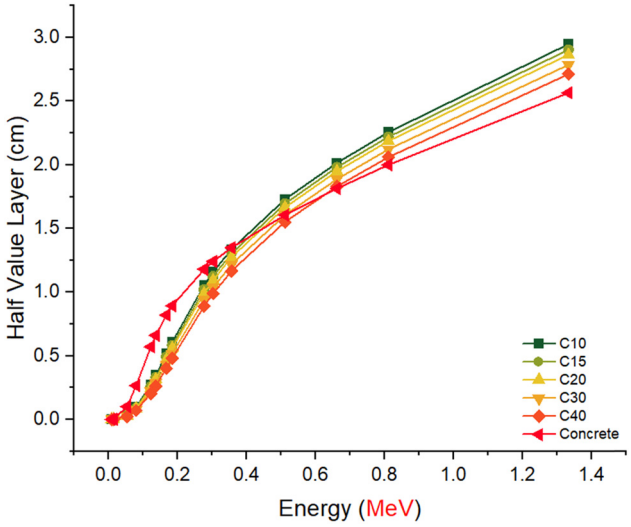

Figure 5: Variations of half value layer (cm) with photon energy (MeV) for all C0–C8 glasses and concrete.

source and prompt identification of any contamination that may occur, allowing required measures to be taken. Nevertheless, implementing the outcomes of this research in practice and expanding the allowable CdO additive quantity to greater levels may be a few critical future studies that may be recommended to scientific community.

Acknowledgments: This work was performed under Princess Nourah bint Abdulrahman University Researchers Supporting Project Number (PNURSP2022R149), Princess Nourah bint Abdulrahman University, Riyadh, Saudi Arabia. Authors express their sincere gratitude to Princess Nourah bint Abdulrahman University.

Funding information: This study was supported by Princess Nourah bint Abdulrahman University Researchers Supporting Project Number (PNURSP2022R149).

Author contributions: Methodology: H.O.T., R.U.E., H.M.H.Z., S.A.M.I., and G.K; software: H.O.T., G.A., H.M.H.Z., and A.E.; validation: S.A.M.I., R.U.E., and A.E.; formal analysis: G.K., D.S.B., H.M.H.Z., and R.U.E.; investigation: G.K. and H.O.T.; resources: G.K., G.A., and H.O.T.; data curation: S.A.M.I. and A.E.; writing – original draft preparation: H.O.T., G.S., G.L., Y.S.R., and G.A; writing – review and editing: H.M.H.Z., S.A.M.I., and A.E.; visualization: D.S.B. and G.K.; supervision: H.M.H.Z. and G.A.; project administration: H.O.T. and R.U.E.; funding acquisition: A.E. (The authors thank the "Dunarea de Jos" University of Galati, Romania, for the APC support.) All authors have read and agreed to the published version of the manuscript.

Conflict of interest: The authors declare no conflict of interest.

Ethical approval: The conducted research is not related to either human or animal use.

Data availability statement: The data presented in this study are available on request from the corresponding author.

References

[1] Fahey FH, Goodking A, Treves ST, Grant FD. Nuclear medicine and radiation protection. J Radiol Nurs. 2016;35(1):5–11.
[2] Treves ST, Fahey FH. Dose optimization in pediatric nuclear medicine. Pediatric Nuclear Medicine and Molecular Imaging. New York: Springer; 2014. pp. 683–94.
[3] Başağaoğlu I. History of cerrahpasa nuclear medicine branch. Turkish J Nucl Med. 1994;3(4):141–4.
[4] Cutler CS, Lewis JS, Anderson CJ. Utilization of metabolic, transport and receptor-mediated processes to deliver agents for cancer diagnosis. Adv Drug Deliv Rev. 1999 Apr;37(1–3):189–211.
[5] Radiation protection and safety of radiation sources: international basic safety standards. IAEA Gen Saf Requir. 2014;3:10–1.
[6] Lukoff J, Olmos J. Minimizing medical radiation exposure by incorporating a new radiation "Vital Sign" into the electronic medical record: Quality of Care and Patient Safety. Perm J. 2017;21:17-007. doi: 10.7812/TPP/17-007.
[7] Applying radiation safety standards in nuclear medicine. Safety reports series no. 40. Vienna: IAEA; 2005.
[8] Relative biological effectiveness (RBE), radiation weighting factor (wR), and quality factor (Q) ICRP Publication 92 (Ann. ICRP 33 (4)); 2003.
[9] Abuzaid MM, Elshami W, Hasan H. Knowledge and adherence to radiation protection among healthcare workers at operation theater. Asian J Sci Res. 2018;12(1):54–9.
[10] Elshami W, Uslu Erdemir R, Abuzaid MM, Cavli B, Issa B, Tekin HO. Occupational radiation dose assessment for nuclear medicine workers in Turkey: A comprehensive investigation. J King Saud Univ Sci. 2002;34:102005. doi: 10.1016/j.jksus.2022.102005.
[11] Adliene D, Griciene B, Skovorodko K, Laurikaitiene J, Puiso J. Occupational radiation exposure of health professionals and cancer risk assessment for Lithuanian nuclear medicine workers. Env Res. 2020 Apr;183:109144.
[12] Al-Abdulsalam A, Brindhaban A. Occupational radiation exposure among the staff of departments of nuclear medicine and diagnostic radiology in Kuwait. Med Princ Pract. 2014;23(2):129–33.
[13] Elshami W, Abuzaid M, Piersson AD, Mira O, AbdelHamid M, Zheng X, et al. Occupational dose and radiation protection practice in uae: a retrospective cross-sectional cohort study (2002–2016). Radiat Prot Dosimetry. 2019 Dec;187(4):426–37.

[14] Elshami W, Abuzaid M, Pekkarinen A, Kortesniemi M. Estimation of occupational radiation exposure for medical workers in radiology and cardiology in the United Arab Emirates: nine hospitals experience. Radiat Prot Dosimetry. 2020 Jul;189(4):466–74.
[15] Elshami W, Akudjedu TN, Abuzaid M, David LR, Tekin HO, Cavli B, et al. The radiology workforce's response to the COVID-19 pandemic in the Middle East, North Africa and India. Radiography. 2021 May;27(2):360–8.
[16] Almatari M, Agar O, Altunsoy E, Kilicoglu O, Sayyed M, Tekin HO. Photon and neutron shielding characteristics of samarium doped lead alumino borate glasses containing barium, lithium and zinc oxides determined at medical diagnostic energies. Results Phys. 2019;12:2123–8.
[17] Tekin HO, ALMisned G, Rammah YS, Susoy G, Ali FT, Baykal DS, et al. Mechanical properties, elastic moduli, transmission factors, and gamma-ray-shielding performances of Bi2O3–P2O5–B2O3–V2O5 quaternary glass system. Open Chem. 2022;20(1):314–29.
[18] Computer Code Collection RS. In MCNPX'User's Manual Version 2.4.0. In Monte Carlo N-Particle Transport Code System for Multiple and High Energy Applications; Oak Ridge National Laboratory: Oak Ridge, TN, USA; Advanced Accelerator Applications Los Alamos National Laboratory: Los Alamos, NM, USA; 2002.
[19] Zhukovsky M, Koubisy MS, Zakaly HM, Ali AS, Issa SA, Tekin HO. Dielectric, structural, optical and radiation shielding properties of newly synthesized CaO–SiO2–Na2O–Al2O3 glasses: experimental and theoretical investigations on impact of Tungsten (III) oxide. Appl Phys, A Mater Sci Process. 2022;128(3):205.
[20] Tekin HO, Susoy G, Issa SA, Ene A, ALMisned G, Rammah YS, et al. Heavy Metal Oxide (HMO) glasses as an effective member of glass shield family: A comprehensive characterization on gamma ray shielding properties of various structures. J Mater Res Technol. 2022;18:231–44.
[21] Deliormanlı AM, Ensoylu M, Issa SA, Rammah YS, ALMisned G, Tekin HO. A thorough examination of gadolinium (III)-containing silicate bioactive glasses: synthesis, physical, mechanical, elastic and radiation attenuation properties. Appl Phys, A Mater Sci Process. 2022;128(4):266.
[22] Rammah YS, Issa SA, Tekin HO, Badawi A, Ene A, Zakaly HM. Binary contributions of Dy3 + ions on the mechanical and radiation resistance properties of oxyfluoroborotellurite Dyx-glasses. J Mater Res Technol. 2022;18:820–9.
[23] Tekin HO, ALMisned G, Issa SA, Zakaly HM. A rapid and direct method for half value layer calculations for nuclear safety studies using MCNPX Monte Carlo code. Nucl Eng Technol. (2022) In Press. doi: 10.1016/j.net.2022.03.037.
[24] Lakshminarayana G, Tekin HO, Dong MG, Al-Buriahi MS, Lee DE, Yoon J, et al. Comparative assessment of fast and thermal neutrons and gamma radiation protection qualities combined with mechanical factors of different borate-based glass systems. Results Phys. 2022;37:105527.
[25] Akkurt I, Tekin HO. Radiological parameters for bismuth oxide glasses using phy-X/PSD Software. Emerg Mater Res. 2020:9(3):1020–102. doi: 10.1680/jemmr.20.00209.
[26] Ozge Kilicoglu HO. Tekin. Bioactive glasses and direct effect of increased K2O additive for nuclear shielding performance: A comparative investigation. Ceram Int. 2020;46(2):1323–33.
[27] Lakshminarayana G, Kumar A, Tekin HO, Issa SA, Al-Buriahi MS, Dong MG, et al. Illustration of distinct nuclear radiation transmission factors combined with physical and elastic characteristics of barium boro-bismuthate glasses. Results Phys. 2021;105067:105067.
[28] Tekin HO, Issa SA, Mahmoud KA, El-Agawany FI, Rammah YS, Susoy G, et al. Nuclear Radiation Shielding Competences of Barium (Ba) Reinforced Borosilicate Glasses. Emerg Mater Res. 2020,4:1–12. doi: 10.1680/jemmr.20.00185.
[29] Lakshminarayana G, Kumar A, Tekin HO, Issa SA, Al-Buriahi MS, Dong MG, et al. In-depth survey of nuclear radiation attenuation efficacies for high density bismuth lead borate glass system. Results Phys. 2021;23:104030.
[30] Hesham MH, Zakaly HA, Issa SA, Rashad M, Elazaka AI, Tekin HO, et al. Alteration of optical, structural, mechanical durability and nuclear radiation attenuation properties of barium borosilicate glasses through BaO reinforcement: experimental and numerical analyses. Ceram Int. 2021;47(4):5587–96.
[31] Kumar A, Gaikwad DK, Obaid SS, Tekin HO, Agar O, Sayyed MI. Experimental studies and Monte Carlo simulations on gamma ray shielding competence of (30 + x)PbOe10WO3e 10Na2O –10MgO – (40-x)B2O3 glasses. Prog Nucl Energy. 2019;119:103047.
[32] Mahmoud IS, Issa SA, Saddek YB, Tekin HO, Kilicoglu O, Alharbi T, et al. Gamma, neutron shielding and mechanical parameters for vanadium lead vanadate glasses. Ceram Int. 2019;45:14058–72.
[33] Uosif MA, Mostafa AM, Issa SA, Tekin HO, Alrowaili ZA, Kilicoglu OJ. Structural, mechanical and radiation shielding properties of newly developed tungstenlithium borate glasses: an experimental study. J Non-Cryst Solids. 2020;532:119882.
[34] Tekin HO, Issa SAM, Mahmoud KA, El-Agawany FI, Rammah YS, Susoy G, et al. Nuclear radiation shielding competences of Barium (ba) reinforced borosilicate glasses. Emerg Mater Res. 2020,4:1–12. doi: 10.1680/jemmr.20.00185.
[35] Kurtulus R, Kavas T, Akkurt I, Gunoglu K, Tekin HO, Kurtulus C. A comprehensive study on novel alumino-borosilicate glass reinforced with Bi2O3 for radiation shielding applications: synthesis, spectrometer, XCOM, and MCNP-X works. J Mater Sci Mater Electron. 2021;32(10):13882–96.